Study on the mechanism of Shenling Baizhu powder on the pathogenesis of pregnancy complicated with non-alcoholic fatty liver, based on PI3K/AKT/mTOR signal pathway

Yao Le,[1,2] Zhijun Wang,[2] Qian Zhang,[2] Ling Miao,[3] Xiaohong Wang,[2] Guorong Han[1]

[1]Department of Gynecology and Obstetrics, The Second Hospital of Nanjing, Nanjing Hospital Affiliated to Nanjing University of Chinese Medicine, Nanjing
[2]Department of Gynecology and Obstetrics, 904 Hospital of the People's Liberation Army joint Logistic Support Force, Wuxi
[3]Department of Gynecology, Wuxi Rehabilitation Hospital, Wuxi, China

ABSTRACT

This study investigates the effectiveness of Shenling Baizhu powder in managing non-alcoholic fatty liver disease (NAFLD) during pregnancy and its mechanism through the PI3K/AKT/mTOR signaling pathway. Eight healthy male and 24 female Sprague-Dawley rats were used. After acclimatization, 6 female rats were fed normal chow, and 18 female rats were fed high-fat chow to induce NAFLD. After 8 weeks, female rats were mated with males to create a pregnant NAFLD model. The rats were divided into four groups: normal feeding, high-fat diet with saline, high-fat diet with 1.6 g/kg Shenling Baizhu powder, and high-fat diet with 4.8 g/kg Shenling Baizhu powder. Maternal body weight, serum and liver levels of aspartate aminotransferase (AST), alanine transaminase (ALT), triglyceride (TG), total cholesterol (TC), low density lipoprotein cholesterol (LDL-C), high density lipoprotein cholesterol (HDL-C), related inflammatory indexes interleukin-1 β (IL-1 β), tumor necrosis factor-α (TNF-α) and interleukin-6 (IL-6) were measured. Liver tissue was examined using hematoxylin eosin, and oil red O staining, and protein expression related to the PI3K/AKT/mTOR pathway was assessed *via* Western blotting, immunohistochemistry and RT-PCR. Results showed significant weight gain and increases in ALT, AST, TG, TC, LDL-C, IL-1β, TNF-α, and IL-6, along with decreased HDL-C in NAFLD rats compared to controls. The high and low-dose Shenling Baizhu powder groups exhibited improvements in body weight, liver histopathology, and reductions in serum TG, TC, LDL-C, ALT, AST, IL-1β, TNF-α, and IL-6, with increased HDL-C levels. Notably, the high-dose group showed greater efficacy in reducing hepatic fat accumulation, liver function markers, blood lipids, and inflammatory indexes, and decreased expression of hepatic PPARγ mRNA, SREBP1 mRNA, AKT mRNA, and related proteins. Shenlin Baizhu powder demonstrates potential in ameliorating high-fat diet-induced NAFLD in pregnant rats, likely through modulation of the PI3K/AKT/mTOR pathway, suggesting its therapeutic potential for gestational NAFLD.

Key words: PI3K/AKT/mTOR; Shenling Baizhu powder; pregnancy; non-alcoholic fatty liver; high-fat diet.

Correspondence: Guorong Han, Department of Gynecology and Obstetrics, The Second Hospital of Nanjing, Nanjing Hospital Affiliated to Nanjing University of Chinese Medicine, 1-1 Zhongfu Road, Gulou District, Nanjing, Jiangsu 210000, China. E-mail: 18262243268@163.com

Contributions: all the authors made a substantive intellectual contribution, performed part of the experiments. All the authors read and approved the final version of the manuscript and agreed to be accountable for all aspects of the work.

Conflict of interest: the authors declare no conflicts of interest related to this work.

Ethics approval: all experiments and the protocol were approved by the ethical committee of 904 Hospital of the People's Liberation Army joint Logistic Support Force (approval no. 20231201).

Availability of data and materials: the data used to support the findings of this study are available from the corresponding author upon request.

Introduction

Non-alcoholic fatty liver disease (NAFLD) is characterized by hepatocyte steatosis exceeding 5%. Although the pathological presentation resembles that of alcoholic fatty liver disease, patients with NAFLD typically consume minimal to no alcohol, instead developing liver steatosis due to alternative factors, resulting in ongoing liver injury. Metabolic stress-induced liver injury is closely linked to obesity, insulin resistance, metabolic syndrome, as well as genetic and lifestyle influences. This association is particularly notable in cases of insulin resistance and genetic predisposition.[1] NAFLD is a prevalent liver disorder globally, impacting approximately 20-30% of the population,[2,3] with a rising incidence observed annually. The incidence of NAFLD in China has reached 32.9%.[4] NAFLD encompasses a diverse clinicopathologic range, from non-alcoholic fatty liver to non-alcoholic steatohepatitis and advancing fibrosis, potentially resulting in end-stage liver conditions such as cirrhosis and hepatocellular carcinoma.[5-7] Research has indicated that mortality rates related to NAFLD increase in the elderly population among both men and women, as well as in specific racial groups.[8] Limited research has been conducted on the impact of NAFLD during pregnancy. Several studies[9-14] have indicated that pregnancy complicated by non-alcoholic fatty liver is linked to negative pregnancy outcomes, including gestational diabetes mellitus, hypertensive disorders, postpartum hemorrhage, low birth weight, and macrosomia. At present, no medications have received approval from the Food and Drug Administration (FDA) or the European Medicines Agency (EMA) for the treatment of NAFLD. However, certain hypoglycemic drugs, as well as other medications such as vitamin E, statins, and pentoxifylline, have demonstrated efficacy in managing NAFLD. Recent research has expanded to include the application of traditional Chinese medicine in the treatment of pregnancy complicated by NAFLD, aiming to enhance therapeutic outcomes. Traditional Chinese medicine is characterized by its ability to target multiple pathways and targets. NAFLD is classified in traditional Chinese medicine as "plumpness", "accumulation", "fatness", "hypochondriac pain" and "liver addiction". Traditional Chinese medicine has demonstrated efficacy in addressing the etiology and clinical manifestations of NAFLD. Shenling Baizhu powder (SLBZ), derived from the prescriptions of peaceful benevolent dispensary, comprises a combination of medicinal ingredients including Ginseng, *Atractylodes macrocephala*, *Poria cocos*, Yam, Semen Coicis, *Lentinus edodes*, Semen Armeniacae, *Platycodonis*, Lotus Root Meat, and *Glycyrrhiza uralensis*. Several of these components are commonly consumed as food in everyday life. The serine/threonine kinase known as mammalian target of rapamycin (mTOR) serves as a pivotal signaling molecule within the cell, governing processes such as cell growth cycle progression, protein synthesis and degradation, membrane protein transport, and protein kinase signaling. The mTOR pathway consisted of two distinct complexes, mTORC1 and mTORC2.[15,16] While mTORC2 was characterized by a relatively straightforward signaling pathway, mTORC1 is recognized for its more significant functional role. Multiple recent studies[17-19] have explored the SLBZ impact on pathways associated with NAFLD, revealing its potential efficacy as a treatment for this condition. The findings underscore the importance of SLBZ in the management of NAFLD. SLBZ exhibit potential in ameliorating symptoms in patients with NAFLD, including reducing blood lipids, alleviating liver inflammation, and preventing fatty liver. Nonetheless, research on NAFLD during pregnancy remains limited.[20,21] Nevertheless, the precise mechanism underlying pregnancy in individuals with NAFLD remains unclear. Hence, our research focused on investigating the potential role of the PI3K/AKT/mTOR signaling pathway in mediating the SLBZ effects on the pathogenesis of NAFLD during pregnancy.

Materials and Methods

Experimental animals

A total of 32 Sprague-Dawley rats, consisting of eight male and 24 female rats, aged 8 weeks and weighing approximately 220 g, were procured from the Experimental Animal Center of Yangzhou University [SCXK (Su) 2022-0009] and used for the experiments after a one-week period of acclimatization to the feeding conditions. The rats were housed in a specific pathogen-free (SPF) environment, the room temperature being 24±2°C, a 12-h light/dark cycle, and humidity maintained between 40-60%. All experiments and the protocol were approved by the Ethical Committee of The 904 Hospital of the People's Liberation Army joint Logistic Support Force (approval number: 20231201), and all operations and handling procedures were conducted in accordance with the National Research Council Guide for the Care and Use of Laboratory Animals.

Modeling method

The control group of rats received a standard basal diet, while the remaining three groups were provided with a high-fat diet in order to induce the NAFLD model.[22] The specific dose of each rat was converted according to the number of animal model system. The high-fat diet consisted of 88% basal feed, 10% lard, 1.5% cholesterol, and 0.5% bile salt. This diet was administered once daily for a duration of 8 weeks. Blood samples were obtained from the orbital veins of six randomly selected female rats that were fed a high-fat diet, as well as six female rats that were fed a normal diet. The levels of TG, TC, ALT, and AST were measured in order to validate the efficacy of the NAFLD model. Female and male rats were housed together in a ratio of 3:1. Daily observations were conducted to detect the presence of a pubic embolus, which confirmed pregnancy and established the NAFLD combined pregnancy model.

Grouping method

The rats were allocated into four groups using random assignment: a control group (receiving normal feeding after cage closure), a model group (receiving a high-fat diet after cage closure and intragastric administration of normal saline), a SLBZ low-dose group (receiving a high-fat diet and 1.6 g/kg intragastric administration of SLBZ), and a SLBZ high-dose group (receiving a high-fat diet and 4.8 g/kg intragastric administration of SLBZ after cage closure). The grouping information was listed in Table 1.

Intervention methods

The model of NAFLD combined with pregnancy was established. The pregnancy combined with NAFLD group and NAFLD group were administered a medicinal solution of SLBZ at a dosage of 10 mL per kilogram of body weight, while the blank group and normal model group received drinking water.

Detection method

Body weight fluctuations in female rats were documented at various stages of gestation. The serological indexes were detected by collecting blood from the heart of female rats prior to euthanasia. The blood was allowed to sit for 4-6 h, and then centrifuged at 12,000 rpm for 20 min, and the resulting supernatant was aspirated. The serum underwent analysis for TG, TC, LDL-C, and HDL-C, as well as ALT, AST, and inflammatory markers including IL-1β, TNF-β, TNF-α, and IL-6, along with the assessment of liver TG and TC levels in the organs.

Histopathological examination of the liver

The liver histopathology involved fixation of tissue in 10% formaldehyde for 48 h, followed by embedding in paraffin and sectioning to a thickness of approximately 4-5 μm. The hematoxylin and eosin (H&E) staining was conducted as per the traditional procedure for dewaxing, involving rehydration, immersion in hematoxylin solution, repeated rinsing, further immersion in eosin solution, and subsequent dehydration. Following sealing, the cells were examined under an OLYMPUS microscope (IX71) and photographed for documentation. Oil Red O staining was performed on tissue that had been embedded in OCT and frozen sectioned at a thickness of approximately 8 μm. The sections were stained with Oil Red O for 30 min, followed by washing of the staining solution. The slices were then sealed with glycerol, examined under a microscope, and photographed.

Immunohistochemistry

Following standard procedures for dewaxing and rehydration, specimens were thoroughly rinsed three times with phosphate-buffered saline (PBS) solution. Subsequently, an antigen retrieval solution was applied, and the specimens were subjected to heat-induced epitope retrieval at 98°C for 20 min. This process used a citrate buffer (pH 6.0) for antigen retrieval. The blocking agent, 3% hydrogen peroxide, was then added dropwise, and the solution was allowed to stand at room temperature for 20 min. The samples were washed by rinsing them three times with PBS. Next, the primary antibody was added at a concentration of 2% bovine serum dilution, and the samples were incubated at either 37°C for 2 h or at 4°C overnight. Following the incubation with the primary antibody, the samples were washed three times with PBS. A secondary antibody solution containing a 2% concentration of bovine serum was then added dropwise. The incubation of the secondary antibody was carried out at 37°C for 1 h, while being shielded from light. After incubation, the washing process was repeated three times with PBS, followed by the addition of 3,3'-diaminobenzidine (DAB) for color development over a period of 15 min. Hematoxylin was applied to counterstain the nuclei for 10 min, followed by dehydration and sealing of the sections. The cells were then examined under a microscope to observe each tissue section. Negative controls were performed by omitting the primary antibody and replacing it with PBS. Details of the antibodies used are provided in Table 2. The immunolabelling was assessed quantitatively by evaluating the staining intensity and the percentage of positive cells. For each sample and condition, at least five randomly selected fields were examined under a microscope at 400x magnification. The stained sections were analyzed using ImageJ software to quantify the staining intensity and the area covered by the staining. This quantitative analysis ensured an objective assessment of the immunolabelling results.

Western blotting

Western blotting was employed to identify variations in protein expression, with the target tissues being isolated using pre-cooled instruments. The tissues were then separated with pre-cooled tools and kept on ice to minimize hydrolysis by protease. Approximately 200 μL of pre-cooled lysate, with protease and phosphatase inhibitors added beforehand, was added per 10 mg of tissue. The homogenization process took place in an ice bath, followed by a 2 h incubation at 4°C with agitation. It was essential for the volume of lysate to correspond to the volume of the tissue sample. The protein sample was centrifuged at 4°C for 12000 rpm for 20 min. The supernatant was carefully aspirated, and the protein sample was subsequently transferred to a fresh, pre-cooled microcentrifuge tube and placed on ice, while the precipitate was discarded. The protein concentration was determined using the BCA method, and protein electrophoresis was performed *via* SDS-PAGE. The transfer of proteins onto the PVDF membrane was conducted using a constant current of 200 mA for approximately 40 min, with variations in transfer time depending on the size of the proteins, typically around 1 min per 1 kD. The PVDF membrane was immersed in a solution containing 5% skimmed milk powder and agitated gently at ambient temperature for a duration of 1 h. Subsequently, the membrane was rinsed and the primary antibody was diluted in the milk powder solution as per the recommended dilution ratios provided in the antibody instructions. The membrane was then incubated at 4°C overnight in a light-protected environment, followed by multiple washes with TBST solution, each lasting 10 min and repeated thrice. The second antibody was diluted to a concentration of 1:2000 using blocking solution, and the PVDF membrane containing the transferred protein was subjected to agitation and incubated for a duration of 2 h. Subsequently, the membrane should be washed with TBST, undergoing a total of 5 washes, each lasting 15 min. Following the washing of the membrane, luminescent liquids (liquid A and liquid B) should be added in a 1:1 ratio, taking care to minimize exposure to light. Using a pipette, the appropriate volume of luminescent liquid should be applied to cover the PVDF membrane. Subsequently, the membrane should be exposed on an ECL luminometer to capture an image.

Table 1. Experimental grouping summary of rats in the study.

Group name	Number of rats	Sex	Diet type	Treatment
Control group	6	Female	Normal chow	None
Model group	6	Female	High-fat diet	Mated with males to induce NAFLD model
SLBZ low group	6	Female	High-fat diet	NAFLD model and administered 1.6 g/kg Shenling Baizhu powder
SLBZ high group	6	Female	High-fat diet	NAFLD model and administered 4.8 g/kg Shenling Baizhu powder

SLBZ, Shenling Baizhu powder.

Table 2. Immunohistochemistry antibodies details.

Primary antibodies	Manufacturer	Article number	Dilution rate	Species	Corresponding secondary antibody	Dilution rate
P-MTOR	Proteintech	67778-1-1g	1:500	M	Servicebio GB23301	1:500
P-PI3K	Affinity	AF3241	1:100	R	Servicebio GB23303	1:500
P-AKT	Cell signaling	4060p	1:100	R	Servicebio GB23303	1:500

RT-PCR detection

Liver tissues of suitable dimensions were obtained and total RNA was isolated utilizing an RNA kit. The total RNA was then extracted using the Vazyme HiScript II Q SuperMix for qPCR Reverse Transcription Kit, followed by reverse transcription using the same kit. Subsequently, PCR amplification was conducted and the results were automatically analyzed using a real-time fluorescence quantitative PCR instrument. The threshold and baseline were calibrated relative to the negative control to ascertain the Ct value for each sample, with the efficacy of the Ct value being assessed based on the melting curve analysis. Subsequently, the relative expression of the target gene mRNA was computed, with the specific primer sequences detailed in Table 3.

Statistical methods

In this research, statistical analysis was conducted using SPSS 27. Means and standard deviations were utilized for continuous variables that followed a normal distribution, while quartile spacing M (Q25, Q75) was employed for continuous variables that did not adhere to a normal distribution. Frequency percentages were used for non-continuous variables, and one-way ANOVA was applied for comparing multiple groups of continuous variables that followed a normal distribution. Variables that do not adhere to a normal distribution were compared across multiple groups using nonparametric tests, and between discontinuous groups using chi-square tests. A significance level of $p<0.05$ was utilized to determine statistical significance. In the figures, CK represents Control group, M represents Model group, Low represents SLBZ low group, High represents SLBZ high group.

Results

Comparison of body weights of rats in each group

The findings of the study revealed that at 8 weeks, the weight of the control group was 311.13±7.26 g, the model group weighed 361.17±10.63 g, the SLBZ low-dose group weighed 363.95±4.07 g, and the SLBZ high-dose group weighed 361.04±3.30 g. Statistical analysis indicated a significant increase in weight in the model group compared to the control group, with a statistically significant difference ($p<0.0001$). The body weights of the SLBZ low- and high-dose groups were found to be comparable to that of the model group, with no statistically significant difference observed. Additionally, within the SLBZ high-dose group, there was no statistically significant variance in body weight when compared to the low-dose group ($p>0.05$) (Figure 1).

Comparison of hepatic steatosis and AST and ALT levels in serum and liver tissues of female rats in each group

The normal liver tissue exhibited a dark brown hue, while the livers of female rats with pregnancy-induced NAFLD displayed a pale, fatty appearance lacking in luster compared to the control group. This observation suggests the successful establishment of pregnancy-induced NAFLD in the female rats (Figure 2). Furthermore, the consecutive administration of both high and low doses of SLBZ significantly improved high-fat diet-induced hepatic pathological changes and restored the healthy appearance of the livers. The histological examination using H&E staining revealed that the liver lobes of the control rats exhibited structural integrity and clarity. The hepatocytes were organized radially around the central vein, with no evidence of hepatocyte swelling or fatty degeneration. Additionally, there was an absence of inflammatory cell infiltration in the confluent area. In the experimental group, the hepatocytes of the rats exhibited predominantly vesicular steatosis and balloon-like lesions, accompanied by inflammatory cell infiltration and occasional scattered punctate necrosis in the confluent area and hepatic sinusoids. The severity of these lesions was reduced in the low-dose group, while in the high-dose group, the lesions more closely resembled those observed in the control group (Figure 3). Additionally, lipid droplet accumulation was verified through Oil Red O staining in the presence of SLBZ high- and low-doses (Figure 4). The findings of this study indicate that

Table 3. PT-RCT primer sequence.

Gene name	Gene sequence 5'-3'
PPARγ RAT-F	GGTGAAACTCTGGGAGATCCT
PPARγ RAT-R	GGTCCACAGAGCTGATTCCG
SREBP1c RAT-F	TTAACGTGGGTCTCCTCCGA
SREBP1c RAT-R	CCAGCATAGGGGGCATCAAA
PPARα RAT-F	GGCTCTGAACATTGGCGTTC
PPARα RAT-R	CAAGGGGACAACCAGAGGAC
Pi3K RAT-F	CCCGAAGGCAGCAGGAG
Pi3K RAT-R	TCACAGCCCCCATTTCAGTC
AKT RAT-F	GAGACGATGGACTTCCGGTC
AKT RAT-R	TGGCAACGATGACCTCCTTC
MTOR RAT-F	GCAATGGGCACGAGTTTGTT
MTOR RAT-R	AGTGTGTTCACCAGGCCAAA
NF-KB- RAT-F	TGCGTTTCCGTTACAAGTGC
NF-KB- RAT-R	GTCTGGATGCGCTGGCTAAT
IKRα- RAT-F	GAAGGCACAGTAACCCCTCC
IKRα- RAT-R	TGCTAACGTCTCGCACACAT
ACTIN-RAT-F	TGGCAACGATGACCTCCTTC
ACTIN-RAT-F	TGGCAACGATGACCTCCTTC

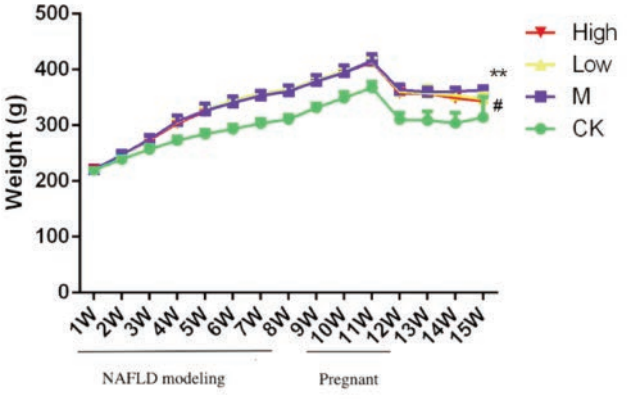

Figure 1. Body weight of mice in each group in different week. CK, control group; M, model group; Low, Shenling Baizhu powder low group; High, Shenling Baizhu powder high group; **$p<0.01$ compared with control group; #$p<0.05$ compared with model group.

female rats in the model group exhibited significantly elevated serum levels of ALT/AST compared to those in the control group (p<0.0001). Furthermore, the liver function of rats in the SLBZ low-dose group, as well as both the low- and high-dose groups, was found to be lower than that of the model group (p=0.014). Notably, the SLBZ high-dose group of demonstrated a more pronounced decrease in liver function (ALT/AST) compared to the low-dose group, with this difference being statistically significant (p<0.0001).

Comparison of serum lipid levels in female rats in each group

The findings of this study indicated that female rats in the model group exhibited significantly elevated serum levels of LDL-C, TC, and TG, as well as significantly reduced HDL-C levels compared to those in the control group (p<0.0001). In comparison to the control group, female rats in the SLBZ low- and high-dose groups exhibited significantly reduced serum levels of LDL-C, TC, and TG, as well as a notable increase in HDL-C levels (p<0.0001). In comparison to the SLBZ low-dose group, the high-dose group of female rats exhibited a significant decrease in serum levels of LDL-C, TC, and TG, along with an elevation in HDL-C levels (p=0.0008). (Figure 5).

Comparison of the levels of inflammatory indices in the serology of female rats in each group

The findings of this study indicate a statistically significant elevation in serum levels of IL-6, IL-1β, and TNF-α in the model group as compared to the control group (p<0.0001). The serum levels of IL-6, IL-1β, and TNF-α in female rats in the SLBZ low- and high-dose groups of exhibited a statistically significant decrease compared to those in the model group (p=0.0484). In comparison to the low-dose, the high-dose group exhibited significantly reduced serum levels of IL-6, IL-1β, and TNF-α (p=0.005) (Figure 6).

Comparison of immunohistochemistry among groups of female rats

In comparison to the control group, the hepatic tissues of female rats in the SLBZ low- and high-dose groups were subjected to immunohistochemistry analysis, revealing a decrease in P-AKT and P-PI3K levels as indicated by assays (p=0.0035). In comparison to the SLBZ low-dose group, the liver tissues of female rats in the high-dose group exhibited a notable reduction, as well as decreased levels of P-AKT and P-PI3K detection (p<0.0001) (Figure 7).

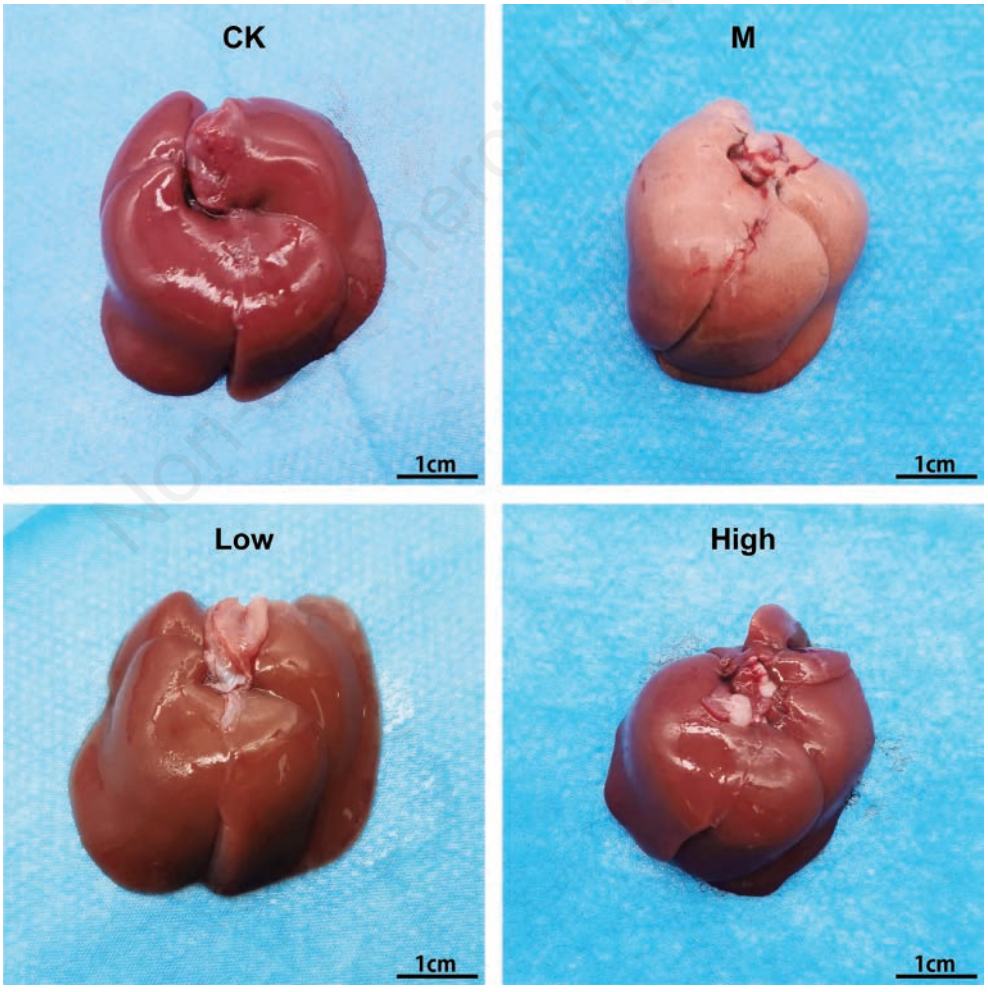

Figure 2. Liver image. CK, control group; M, model group; Low, Shenling Baizhu powder low-group; High, Shenling Baizhu powder high-group.

Comparison of liver protein levels of p-mTOR/mTOR, p-pi3k/pi3k, and P-AKT/AKT in female rats of each group

The findings of this study indicate that there was a statistically significant increase in the protein levels of p-mTOR/mTOR, p-pi3k/pi3k, and P-AKT/AKT in female rats within the model group as opposed to the control group (p=0.0057). In comparison to the control group, the concentrations of p-mTOR/mTOR, p-pi3k/pi3k, and P-AKT/AKT proteins were found to be notably reduced in female rats administered SLBZ low- and high-doses (p=0.0221). In comparison to the low-dose group, the high-dose group of female rats exhibited a significant decrease in protein levels of p-mTOR/mTOR, p-pi3k/pi3k, and P-AKT/AKT (p=0.0041) (Figure 8 A,B).

Comparison of mRNA expression levels of hepatic genes in female rats in each group

The findings of this study indicate that there was a statistically

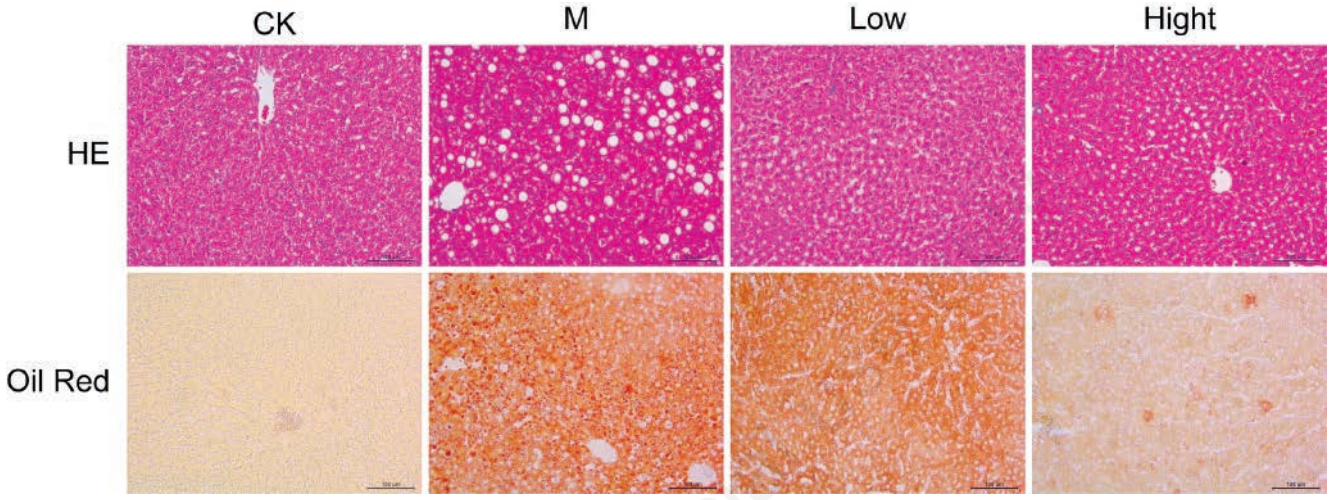

Figure 3. H&E staining and Oil Red O staining of liver sections of different group of rats.

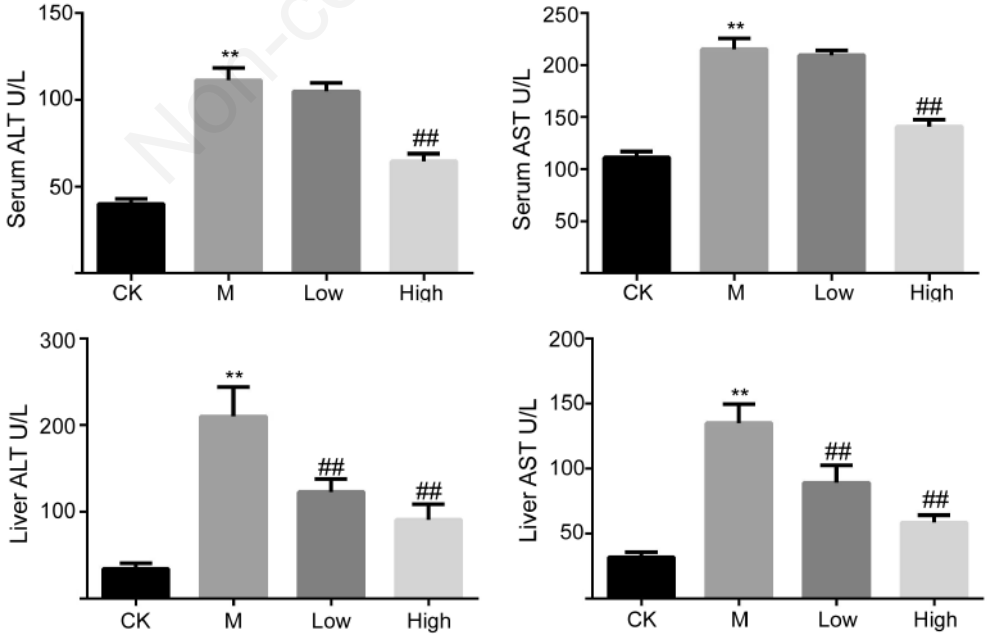

Figure 4. Level of ALT and AST in serum and liver tissue. **p<0.01 compared with control group; ##p<0.01 compared with model group.

significant increase in the expression levels of PPARγ mRNA, SREBP1 mRNA, PPARα mRNA, PI3K mRNA, AKT mRNA, NF-κB mRNA and IKRα mRNA in the female rat model group compared to the control group (p<0.0001). In comparison to the control group, female rats in the SLBZ low- and high-dose groups exhibited significantly reduced expression levels of PPARγ mRNA, SREBP1 mRNA, PPARα mRNA, PI3K mRNA, AKT mRNA, NF-κB mRNA and IKRα mRNA (p=0.0058). In comparison to the SLBZ low-dose group, the high-dose group of female rats exhibited a significant decrease in the expression levels of PPARγ mRNA, SREBP1 mRNA, PPARα mRNA, PI3K mRNA, AKT mRNA, NF-κB mRNA and IKRα mRNA (p=0.0076) (Figure 9).

Discussion

Our study aimed to investigate the effects of a high-fat diet on the development of NAFLD in pregnant rats and to evaluate the therapeutic potential of SLBZ. This research contributes to the understanding of NAFLD's impact during pregnancy and explores a traditional Chinese medicine approach to its management. Our findings indicate that a successful model of combined NAFLD during pregnancy can be achieved using a maternal rat model fed a high-fat diet. This study also demonstrated that SLBZ effectively improved lipid metabolism in the model group.

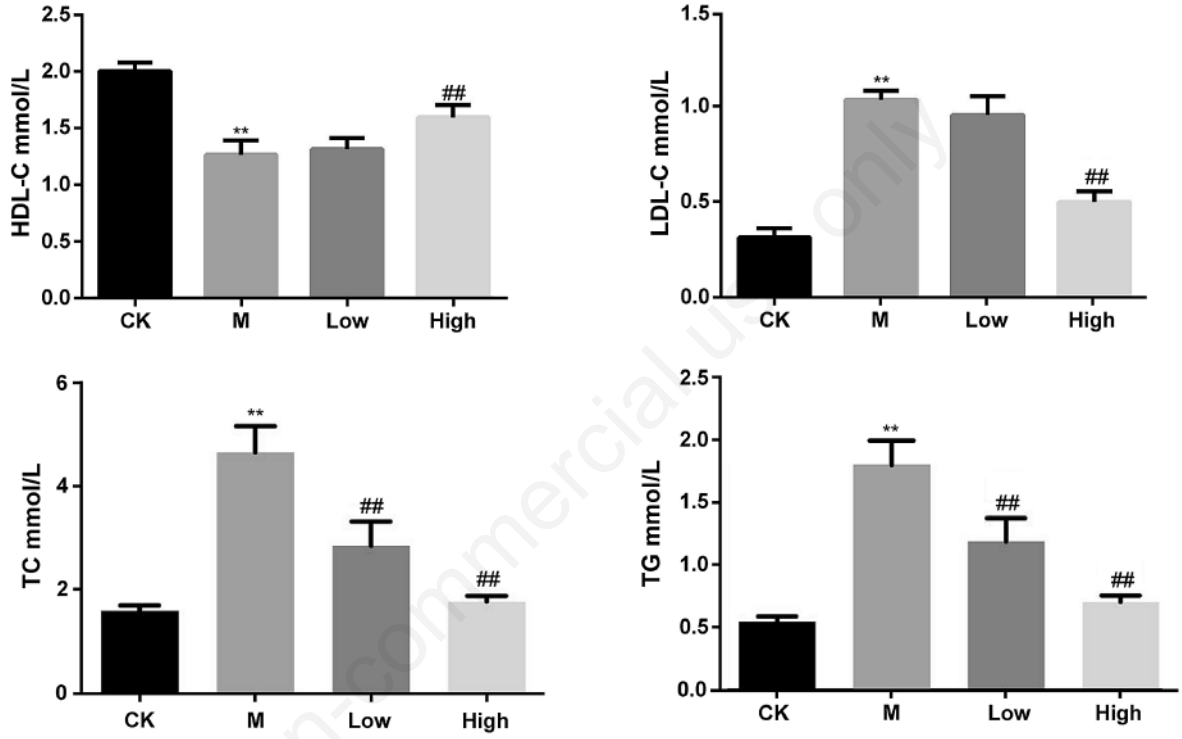

Figure 5. Comparison of the effects of Shenling Baizhu powder on serum lipids in NAFLD female rats. **p<0.01 compared with control group; ##p<0.01 compared with model group.

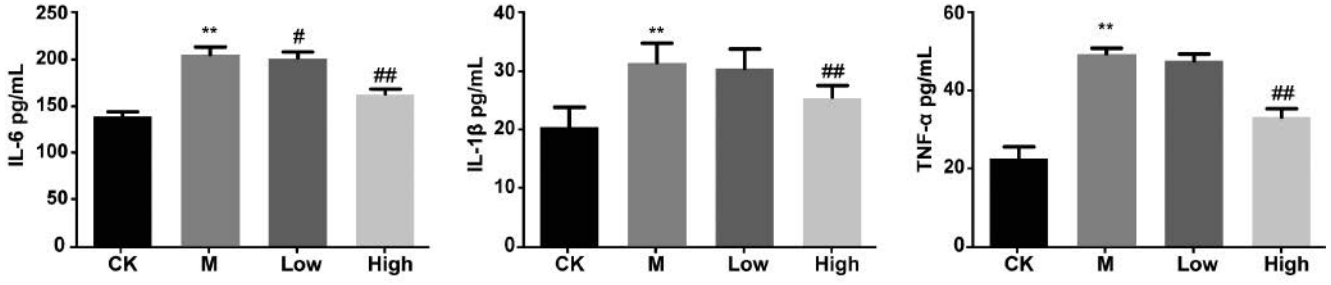

Figure 6. Comparison of the effects of Shenling Baizhu powder on the concentration of IL-6, IL-1 β and TNF- α in serum of NAFLD female rats (pg/mL). **p<0.01 compared with control group; #p<0.05, ##p<0.01 compared with model group.

NAFLD, also known as metabolic dysfunction-associated fatty liver disease, was widely recognized as the hepatic manifestation of the metabolic syndrome.[22,23] NAFLD was intricately linked with obesity, glucose-lipid metabolism, dyslipidemia, and hypertension, among other conditions, and may manifest prior to their onset. This temporal relationship highlights the potential of NAFLD as an early indicator for preventing various metabolic disorders. [23] A previous report examined the SLBZ impact on the liver ultrastructure and mTOR, STAT3 protein phosphorylation in rats with NAFLD.[24] Their findings suggest that SLBZ could enhance the condition of rats in the model group, leading to a notable decrease in liver function levels. They also showed that female rats administered a high-fat diet following SLBZ instillation experienced a significant decrease in body weight and improvement in liver function as evidenced by reductions in AST and ALT levels in both serum and liver tissues. Furthermore, these effects were more pronounced with higher drug concentrations and are consistent with previous research findings.

The lipid ratios TG/HDL-C and TC/HDL-C, established as prognostic indicators of NAFLD severity,[25] were found to be elevated in our high-fat diet-fed rats, correlating with increased risk for disease progression. This is consistent with the work of Arakawa *et al.,*[26] who identified a significant association between inflammatory cytokines TNF-α, IL-1β, and IL-8 and NAFLD progression. Our study further demonstrates that SLBZ intervention not only improves lipid profiles but also modulates inflammatory markers, as evidenced by reduced serum levels of IL-6, IL-1β, and TNF-α. Cai *et al.*[27] conducted a study to examine the therapeutic mechanism of SLBZ in modulating the TLR4/NLRP3 pathway in alcoholic liver disease. The findings indicated that SLBZ was effective in reducing hepatic lipid deposition, improving hepatic function, and mitigating inflammatory responses in hepatic tissue. Our findings parallel these results, with Oil Red O staining confirming the amelioration of hepatic steatosis following SLBZ treatment. Notably, treatment with SLBZ intervention resulted in improvements in lipid profiles and inflammatory markers. Lipid droplet accumulation and hepatic lesion-like hepatic steatosis are observable through Oil Red O staining of liver tissue. SLBZ effectively ameliorated the lipid profile of female rats subjected to a high-fat diet, resulting in notable improvements in hepatic steatosis through reductions in triglyceride, total cholesterol, and low-density lipoprotein cholesterol levels, as well as a decrease in hepatic inflammation.[28]

The modulation of genes within the PI3K/AKT/mTOR signaling pathway, pivotal in lipid homeostasis, was significantly altered in our study's high-fat diet-fed rats. The downregulation of these

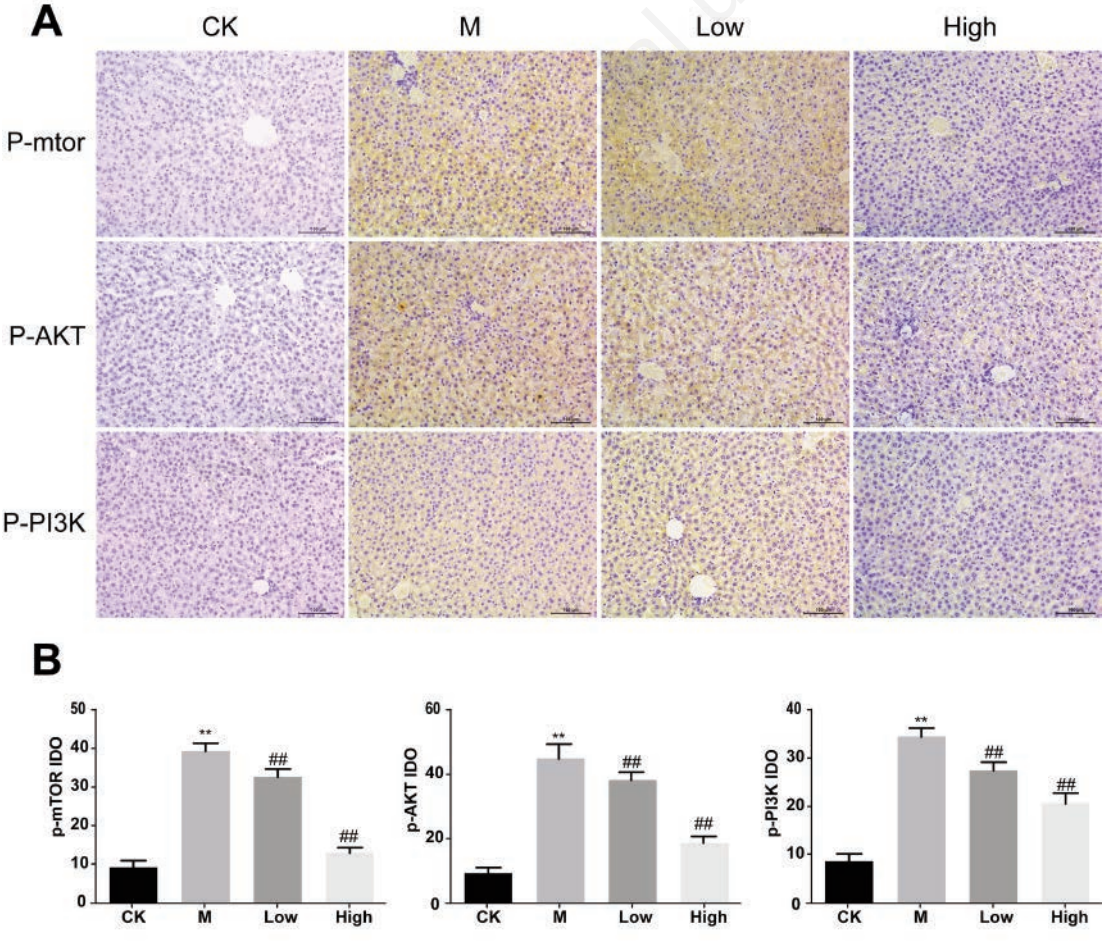

Figure 7. Immunohistochemical detection of liver tissue of PI3K/AKT/mTOR signaling pathway. **p<0.01 compared with control group; ##p<0.01 compared with model group.

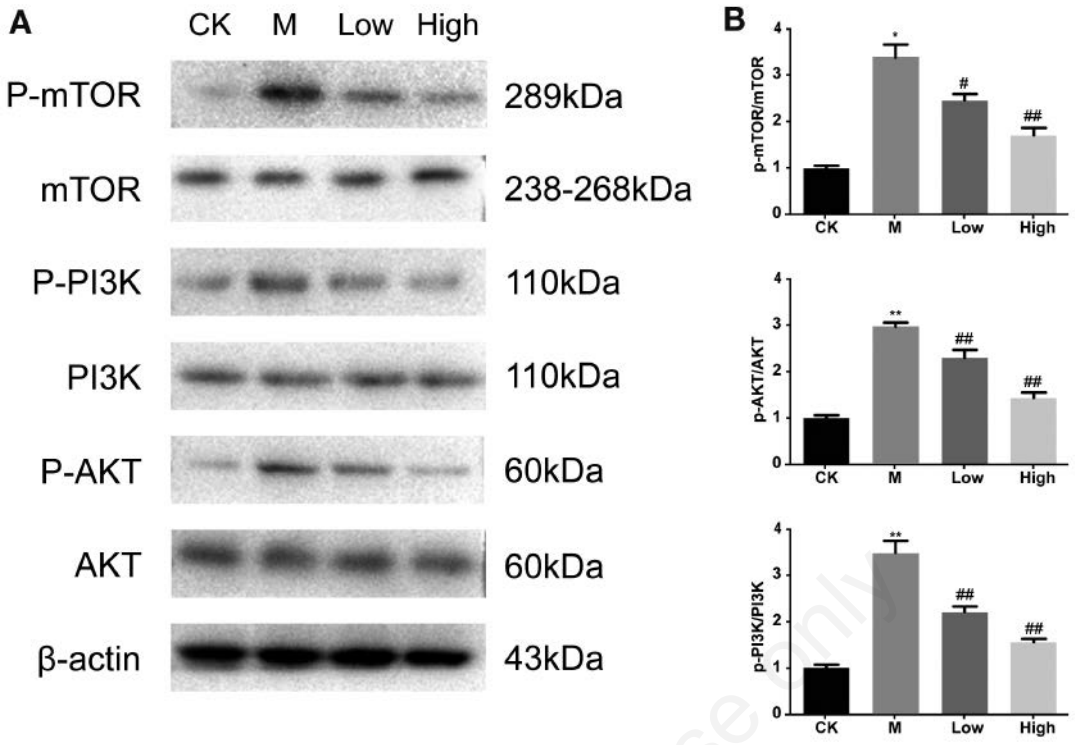

Figure 8. A) The hepatic PI3K/AKT/mTOR protein and mRNA expression. **B**) Western blot analysis of the expression of PI3K/AKT/mTOR signal pathway. *p<0.05, **p<0.01 compared with control group; $^{\#}p$<0.05, $^{\#\#}p$<0.01 compared with model group.

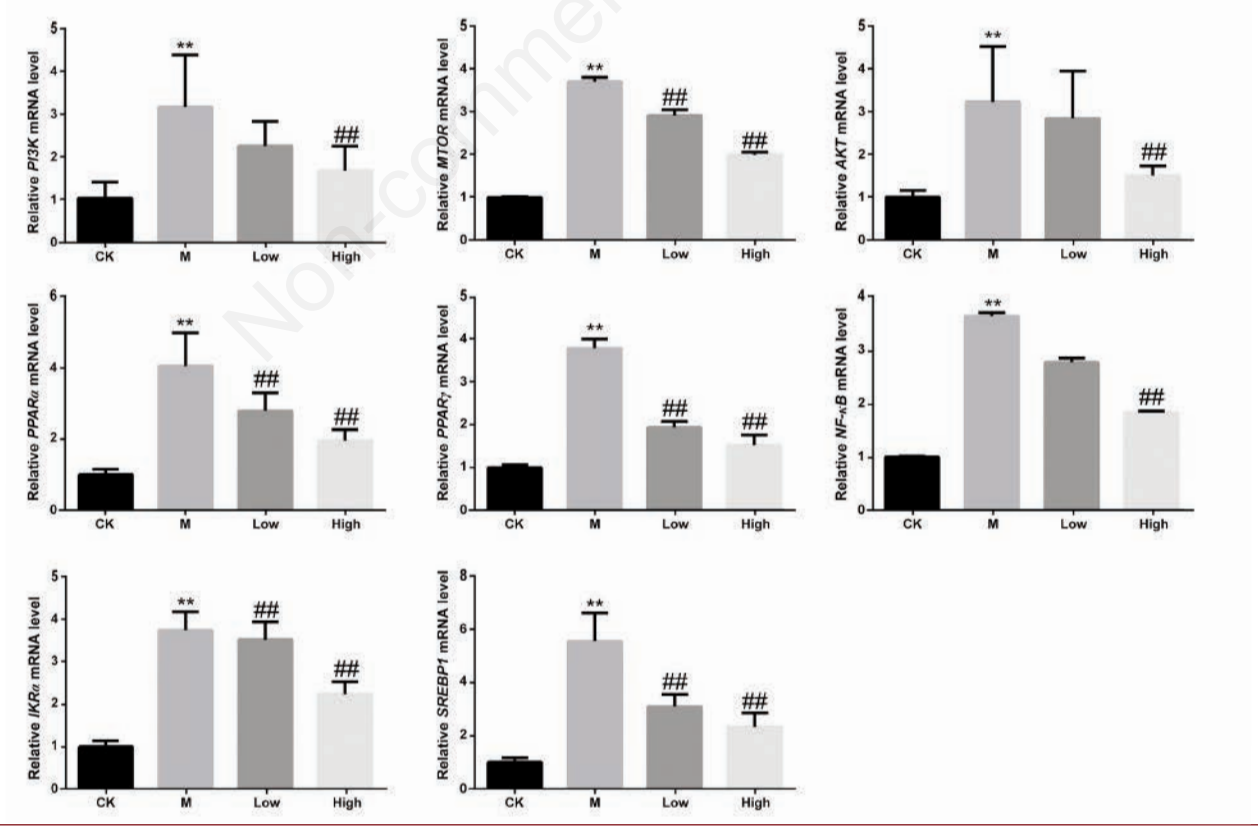

Figure 9. PT-PCR detection and comparison of protein expression of PI3K/ AKT/ mTOR signaling pathway. **p<0.01 compared with control group; $^{\#\#}p$<0.01 compared with model group.

genes, including PPARγ[29] and SREBP1, suggests a potential mechanism by which SLBZ exerts its therapeutic effects. The role of PPARγ in mitigating hepatocellular injury and the regulatory function of SREBP-1 in lipid synthesis are well-documented, as exemplified by the study of Chyau *et al.*[30] on Antrodan's impact *via* the AMPK/Sirt1/CREBP-1c/PPARγ pathway.

Despite the promising results, our study acknowledges several limitations. Firstly, the use of a traditional Chinese medicine compound formula necessitates additional exploration of its specific active ingredients through pharmacological studies. Secondly, the potential effects of traditional Chinese medicine on NAFLD involving multiple pathways and targets require further validation in future research. Lastly, as this study primarily consists of *in vivo* experiments, the mechanisms underlying the impact of SLBZ on NAFLD during pregnancy should be confirmed through subsequent *in vitro* experiments.

In conclusion, the current research has shown that SLBZ exerts a protective influence on NAFLD during pregnancy. The potential mechanism of action appears to be associated with the PI3K/AKT/mTOR pathway, offering a foundation for further investigation into the pathogenesis and treatment targets of NAFLD in pregnancy.

References

1. Rinella ME, Neuschwander-Tetri BA, Siddiqui MS, Abdelmalek MF, Caldwell S, Barb D, et al. AASLD Practice Guidance on the clinical assessment and management of nonalcoholic fatty liver disease. Hepatology 2023;77:1797-835.
2. Younossi ZM, Stepanova M, Younossi Y, Golabi P, Mishra A, Rafiq N, et al. Epidemiology of chronic liver diseases in the USA in the past three decades. Gut 2020;69:564-8.
3. Younossi ZM, Golabi P, Paik JM, Henry A, Van Dongen C, Henry L. The global epidemiology of nonalcoholic fatty liver disease (NAFLD) and nonalcoholic steatohepatitis (NASH): a systematic review. Hepatology 2023;77:1335-47.
4. Zhou J, Zhou F, Wang W, Zhang XJ, Ji YX, Zhang P, et al. Epidemiological features of NAFLD from 1999 to 2018 in China. Hepatology 2020;71:1851-64.
5. Agyapong G, Dashti F, Banini BA. Nonalcoholic liver disease: epidemiology, risk factors, natural history, and management strategies. Ann NY Acad Sci 2023;1526:16-29.
6. Simon TG, Roelstraete B, Khalili H, Hagstrom H, Ludvigsson JF. Mortality in biopsy-confirmed nonalcoholic fatty liver disease: results from a nationwide cohort. Gut 2021;70:1375-82.
7. Rinella ME. Nonalcoholic fatty liver disease: a systematic review. JAMA 2015;313:2263-73.
8. Ilyas F, Ali H, Patel P, Sarfraz S, Basuli D, Giammarino A, et al. Increasing nonalcoholic fatty liver disease-related mortality rates in the United States from 1999 to 2022. Hepatol Commun 2023;7:e00207.
9. Herath RP, Siriwardana SR, Ekanayake CD, Abeysekara V, Kodithuwakku S, Herath HP. Non-alcoholic fatty liver disease and pregnancy complications among Sri Lankan women: A cross sectional analytical study. PLoS One 2019;14:e0215326.
10. Sarkar M, Grab J, Dodge JL, Gunderson EP, Rubin J, Irani RA, et al. Non-alcoholic fatty liver disease in pregnancy is associated with adverse maternal and perinatal outcomes. J Hepatol 2020;73:516-22.
11. Kubihal S, Gupta Y, Shalimar, Kandasamy D, Goyal A, Kalaivani M, et al. Prevalence of non-alcoholic fatty liver disease and factors associated with it in Indian women with a history of gestational diabetes mellitus. J Diabetes Invest 2021;12:877-85.
12. Koralegedara IS, Warnasekara JN, Dayaratne KG, De Silva FN, Premadasa JK, Agampodi SB. Non-alcoholic fatty liver disease (NAFLD): a significant predictor of gestational diabetes mellitus (GDM) and early pregnancy miscarriages-prospective study in Rajarata Pregnancy Cohort (RaPCo). BMJ Open Gastroenter 2022;9:e000831.
13. Gong XW, Xu YJ, Yang QH, Liang YJ, Zhang YP, Wang GL, et al. Effect of soothing Gan (liver) and invigorating Pi (spleen) recipes on TLR4-p38 MAPK pathway in Kupffer cells of non-alcoholic steatohepatitis rats. Chin J Integr Med 2019;25:216-24.
14. El JH, Eslick GD, Weltman M. Systematic review with meta-analysis: non-alcoholic fatty liver disease and the association with pregnancy outcomes. Clin Mol Hepatol 2022;28:52-66.
15. Saxton RA, Sabatini DM. mTOR signaling in growth, metabolism, and disease. Cell 2017;168:960-76.
16. Wei X, Luo L, Chen J. Roles of mTOR signaling in tissue regeneration. Cells 2019;8:1075.
17. Yao Z, Guo J, Du B, Hong L, Zhu Y, Feng X, et al. Effects of Shenling Baizhu powder on intestinal microflora metabolites and liver mitochondrial energy metabolism in nonalcoholic fatty liver mice. Front Microbiol 2023;14:1147067.
18. Qiao B, Xiao N, Deng N, Tan Z. Shenling Baizhu powder attenuates lard diet in a fatigued state-induced diarrhea via targeting microbial metabolites short chain fatty acids-mediated lipid metabolism. 3 Biotech 2024;14:203.
19. Wu P, Wang Y, Ye Y, Yang X, Huang Y, Ye Y, et al. Liver biomarkers, lipid metabolites, and risk of gestational diabetes mellitus in a prospective study among Chinese pregnant women. BMC Med 2023;21:150.
20. Pan M, Deng Y, Qiu Y, Pi D, Zheng C, Liang Z, et al. Shenling Baizhu powder alleviates non-alcoholic fatty liver disease by modulating autophagy and energy metabolism in high-fat diet-induced rats. Phytomedicine 2024;130:155712.
21. Prasomthong J, Limpeanchob N, Daodee S, Chonpathompikunlert P, Tunsophon S. Hibiscus sabdariffa extract improves hepatic steatosis, partially through IRS-1/Akt and Nrf2 signaling pathways in rats fed a high fat diet. Sci Rep 2022;12:7022.
22. Eslam M, Sanyal AJ, George J. MAFLD: a consensus-driven proposed nomenclature for metabolic associated fatty liver disease. Gastroenterology 2020;158:1999-2014.
23. Heindel JJ, Blumberg B, Cave M, Machtinger R, Mantovani A, Mendez MA, et al. Metabolism disrupting chemicals and metabolic disorders. Reprod Toxicol 2017;68:3-33.
24. Chen D, Wang Y, Yang J, Ou W, Lin G, Zeng Z, et al. Shenling Baizhu San ameliorates non-alcoholic fatty liver disease in mice by modulating gut microbiota and metabolites. Front Pharmacol 2024;15:1343755.
25. Cusi K, Isaacs S, Barb D, Basu R, Caprio S, Garvey WT, et al. American Association of Clinical Endocrinology Clinical Practice Guideline for the diagnosis and management of non-alcoholic fatty liver disease in primary care and endocrinology clinical settings: co-sponsored by the American Association for the Study of Liver Diseases (AASLD). Endocr Pract 2022;28:528-62.
26. Arakawa Y, Miyazaki K, Yoshikawa M, Yamada S, Saito Y, Ikemoto T, et al. Value of the CRP-albumin ratio in patients with resectable pancreatic cancer. J Med Investig 2021;68:244-55.
27. Cai SQ, Zhou SF, Zhou LF, Li YR, Zhou XY, Lyu FY. [Mechanism of Shenling Baizhu Powder on treatment of alcoholic liver disease by regulating TLR4/NLRP3 pathway].[Article in Chinese]. Zhongguo Zhong Yao Za Zhi 2024;49:1275-85.

28. Zhu W, Yan M, Cao H, Zhou J, Xu Z. Effects of Clostridium butyricum capsules combined with rosuvastatin on intestinal flora, lipid metabolism, liver function and inflammation in NAFLD patients. Cell Mol Biol 2022;68:64-9.
29. Fan N, Peng L, Xia Z, Zhang L, Song Z, Wang Y, et al. Triglycerides to high-density lipoprotein cholesterol ratio as a surrogate for nonalcoholic fatty liver disease: a cross-sectional study. Lipids Health Dis 2019;18:39.
30. Chyau CC, Wang HF, Zhang WJ, Chen CC, Huang SH, Chang CC, et al. Antrodan alleviates high-fat and high-fructose diet-induced fatty liver disease in C57BL/6 mice model via AMPK/Sirt1/SREBP-1c/PPARgamma pathway. Int J Mol Sci 2020;21:360.

Received: 19 June 2024. Accepted: 2 September 2024.

European Journal of Histochemistry 2024; 68:4093
doi:10.4081/ejh.2024.4093